Dynamics of the activated dissociative chemisorption of N_2 on W(110): A molecular beam study

H. E. Pfnür, C. T. Rettner, J. Lee, R. J. Madix, and D. J. Auerbach

Citation: The Journal of Chemical Physics **85**, 7452 (1986);
View online: https://doi.org/10.1063/1.451334
View Table of Contents: http://aip.scitation.org/toc/jcp/85/12
Published by the American Institute of Physics

Dynamics of the activated dissociative chemisorption of N_2 on W(110): A molecular beam study

H. E. Pfnür,[a] C. T. Rettner, J. Lee,[b] R. J. Madix,[c] and D. J. Auerbach
IBM Almaden Research Center, Department K33/801, San Jose, California 95120-6099

(Received 16 June 1986; accepted 3 September 1986)

Molecular beam techniques have been used to study the dissociative chemisorption of nitrogen on W(110). Chemisorption probabilities have been measured as a function of incidence angle θ_i and kinetic energy E_i surface coverage and temperature. In addition, angular scattering distributions have been measured for a range of conditions and LEED has been used to examine surface structure. The initial (zero coverage limit) sticking probability is found to depend strongly on the incidence energy, scaling approximately with E_i, rather than with the velocity component normal to the surface. This probability is $\leqslant 3\times10^{-3}$ for $E_i \leqslant 30$ kJ mol^{-1}, and rises by more than a factor of 100 by ~ 100 kJ mol^{-1}, where it levels off at ~ 0.35. It is argued that this behavior arises due to a strong chemical interaction prior to the barrier to dissociation. Angular scattering distributions revealed predominately quasispecular scattering with evidence as well for a diffuse component at low energies. The sticking probability falls steadily with increasing surface coverage and a saturation coverage of ~ 0.25 atomic ML is observed for $E_i \sim 10$ kJ mol^{-1}. At higher incidence kinetic energies, this saturation coverage increases to ~ 0.5 ML at 200 kJ mol^{-1}. LEED structures are also reported, corresponding to coverages of 0.25, 0.3, 0.5, and 0.52 ML. The 0.25 and 0.5 ML structures are identified as $p(2\times2)$ and $c(4\times2)$, respectively, for which structure models are proposed.

I. INTRODUCTION

Activated dissociative chemisorption is among the simplest classes of surface chemical reactions. The presence of an activation barrier to adsorption in some sense simplifies the task of understanding such reactions since the dynamics may be dominated by a relatively small region of the potential hypersurface. Even for this case however, there exists no consistent model of the elementary steps involved. Interest in such reactions dates back to Lennard-Jones[1] who proposed that thermally activated adsorption could be understood in terms of a barrier between the potential curve describing the weak molecular interaction experienced initially by an incoming molecule, and that of the strong chemical interaction of the final product. A number of previous molecular beam studies have indicated that this barrier may be essentially one dimensional. The dependence of activated dissociative chemisorption on incidence kinetic energy E_i and angle θ_i has been examined for H_2 and D_2 on a number of Cu surfaces[2-4] for CH_4[5] and O_2[6] chemisorbing on W(110) and for CO_2 on Ni(100).[7] In each case, the chemisorption probability was found to scale with the quantity $E_n = E_i \cos^2\theta_i$; the so-called "normal kinetic energy." Studies of surface recombination have also been successfully accounted for in terms of this one-dimensional barrier (1DB) picture. These include the observation of noncosine angular distributions and non-Boltzmann kinetic energy distributions of molecules which recombine and desorb.[3,4,8,9]

The 1DB model has not been completely successful at treating all aspects of the available data, however. In post-permeation desorption experiments, Comsa and co-workers have observed similar velocity distributions for a range of desorption angles out to $\sim 60°$ from the surface normal, whereas the 1DB model would predict a steep increase in mean velocity with increasing angle.[10] In addition, the observation of populations of excited vibrational states in excess of the Boltzmann value[11,12] are not accounted for. Furthermore, recent experimental[13] and theoretical[14] studies show that deviations from a cosine angular distribution of desorbing particles do not necessarily require activation barriers.

Recently Cosser *et al.*[15] reported observations of angular resolved thermal desorption of N_2 from W(310) and W(110). For the W(310) surface they observed a pure cosine angular distribution of the desorbing particles. However, the distribution from the W(110) surface was found to peak sharply along the surface normal. This was interpreted in terms of a one-dimensional activation barrier, yielding a barrier height of 17.4 kJ mol^{-1} for this surface. These workers pointed out that only $\sim 0.3\%$ of molecules in a 300 K effusive beam have more than this energy, in remarkably good agreement with the measured sticking probability of 3×10^{-3} for such a beam on the clean surface.[16-18] These data implied two intriguing predictions: that the dissociative desorption of N_2 on W(110) might proceed by way of a one-dimensional translational barrier, and that the translational energy dependence might be relatively sharp, corresponding to a barrier height of about 17 kJ mol^{-1}.

Motivated by these results, we have examined the dissociative chemisorption probability of N_2 on W(110) as a function of incidence kinetic energy, as reported previously.[19-21] The kinetic energy dependence for 45° incidence an-

[a] Present address: Fakultät für Physik der TU München, Physikdepartment E20, James Franck Str., D-8046 Garching, West Germany.
[b] Present address: Department of Chemical Technology, College of Engineering, Seoul National University, South Korea.
[c] Present address: Department of Chemical Engineering, Stanford University, Stanford, CA 94305.

 0021-9606/86/247452-15$02.10

gle was found to be consistent with a considerably higher activation barrier (~ 40 kJ mol^{-1}) than indicated by the desorption experiments and displayed a pronounced activation threshold of ~ 20 kJ mol^{-1}, assuming a 1DB model in both cases.[19,20] In addition, the saturation coverage was found to increase with increasing energy and new binding states were observed at high collision energies.[20]

These studies have been extended to other angles of incidence, and in this paper we present the dependence of the chemisorption probability on incidence kinetic energy for incidence angles between 0° and 60°. Our data are found to be completely inconsistent with normal energy scaling, displaying reasonably good scaling with the total translational energy, E_i. A brief report of this data appeared recently.[21] Here we present a full report of this work, together with the results of angular distribution measurements near zero coverage and LEED structure observations for coverages up to 0.52 ML.

II. EXPERIMENTAL APPARATUS AND PROCEDURES

The experimental apparatus consists of a UHV chamber and molecular beam source, as shown in Fig. 1. Various aspects of this machine have been reported previously.[5,19–23] The main chamber has a volume of ~ 320 ℓ and is pumped by a diffusion pump (Edwards, E06), liquid nitrogen trap (Vacuum Generators, CCT 150), and a titanium sublimator (Varian, 922-0032). After bakeout for 24 h at 200 °C typical base pressures of $\lesssim 3\times 10^{-11}$ Torr are obtained. The molecular beam source is demountable and is removed during bakeout.

Experiments are performed with a supersonic beam of N_2 incident on a W(110) single crystal mounted on a rotatable manipulator which is rotated to vary the beam–surface incidence angle. This angle can be read and repositioned to $\lesssim 0.1°$; the absolute value is determined to $\lesssim 0.2°$ using He scattering. Most of the experiments reported here were performed on a sample which was $1.4 \pm 0.5°$ off of the {110} direction. Towards the end of this study the crystal was reoriented to within 0.5° of this direction. Sticking probability and angular distribution measurements were repeated and found to be insensitive to this change. Both sides were polished by standard techniques. The crystal was mounted on the axis of the manipulator by two short tantalum wires spot-welded to the back side of the crystal. The surface normal could be aligned parallel to the molecular beam axis by using a telescope aligned with the beam by a second rotation on the manipulator.

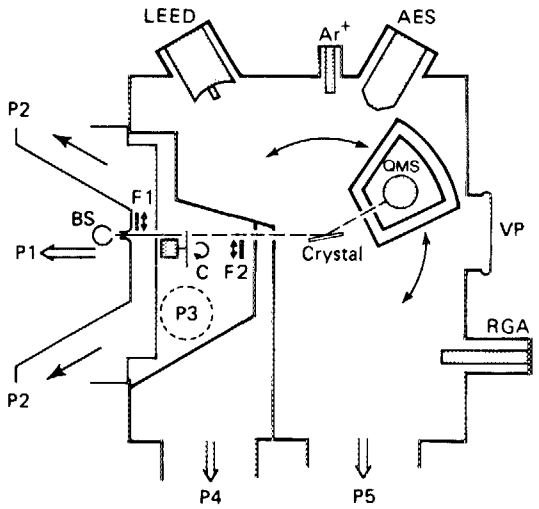

FIG. 1. Molecular beam apparatus for determining scattering distributions and dissociative chemisorption probabilities. Key: P1–P5, pumping stages; BS, beam source; C, chopper; F1 and F2, beam flags; QMS, doubly differentially pumped quadrupole mass spectrometer; LEED, low energy electron diffraction screen; Ar +, argon ion sputtering gun; AES, Auger electron spectrometer; VP, 6 in. viewpoint; RGA, residual gas analyzer. The molecular beam system can detach at the P3 region and is nonbakeable. The crystal is held on a manipulator which provides for heating and cooling and rotates about the same axis as the QMS.

The sample could be heated by electron bombardment to 2500 K and the sample mount cooled with liquid nitrogen. Cleaning was done by extensive heating/cooling cycles between 1550 and 1950 K while the sample was exposed to oxygen with a capillary doser (equivalent pressure of $\sim 1\times 10^{-7}$ Torr at the surface) until, after heating the crystal several times in vacuum to 2500 K impurity levels (mainly carbon) were below the detection limit of our Auger spectrometer (Physical Electronics Industries, 11-500 A). Temperature, monitored with a W–5% Re/W–26% Re thermocouple spot-welded to the edge of the sample, was controlled by a temperature controller (Linear Research, LR-130) interfaced to a minicomputer (IBM, Series 1). This enabled the temperature to be held constant or linearly ramped while maintaining an accuracy ~ 5 K at all times.

All measurements reported here were carried out at a surface temperature of 800 K in order to keep the surface free of hydrogen. At this temperature, no effect could be found by replacing the H_2 seed gas by He, for a given N_2 kinetic energy.

Angular distributions of the scattered N_2 are recorded with a rotatable doubly differentially pumped quadrupole mass spectrometer (Extranuclear Laboratories). This rotates about a vertical axis passing through the crystal surface. The beam and mass spectrometer collimation is such as to yield an effective angular resolution of $\sim 2°$ for molecules scattered in a horizontal plane containing the beam and the surface normal. This detector can be placed on the beam axis for beam characterization. A high-speed chopper driven by a synchronous motor (Globe-TRW, 75A6000) permits beam energies to be determined via time-of-flight measurements. In an earlier stage of the experiment a stationary QMS in line of sight with the molecular beam was used for TOF measurements.

Beam energies for N_2 can be varied between 10 and 220 kJ mol^{-1} by changing the ratio of N_2 to H_2 or He seed gases and by changing the nozzle temperature. The actual mean kinetic energy of N_2 is determined by time-of-flight measurements. These are referenced to a start signal from a photodiode illuminated by an incandescent bulb. This shines through a chopper slit which is 180° from the slit through which the molecular beam passes. The zero time calibration has been established by shining a He/Ne laser along the beam axis and recording the actual shutter function of the

chopper slit compared to a reference photodiode pulse. In addition, it is necessary to allow for the ion flight time to the electron multiplier detector following ionization. Ion flight times have been calibrated using molecular beams of SF_6 and CF_4, comparing the time of arrival peaks of the various mass fragments. All ion flight times, t_{ion}, are consistent with the relation $t_{ion} \sim 3.7 \times M_{ion}^{0.5}$ μs, where M_{ion} is the ion mass.

Beam fluxes, F_x (molecules/cm^2/s), are estimated for species x by measuring the partial pressure increase in the scattering chamber, ΔP (Torr), caused by the beam, measured on a residual gas analyzer (Vacuum Generators, SX200). To avoid interference with contributions from CO, the N_2 signal was monitored at mass 14 in all cases. At steady state

$$F_x = \frac{\Delta P_x S_x N_T}{A_b}, \tag{1}$$

where S_x (cm^3/s) is the system pumping speed for species x, A_b (cm^2) is the effective beam area at the crystal, and $N_T \sim 3 \times 10^{16}$ is the number of molecules per cm^3 at 1 Torr. The beam area at the sample was estimated by moving a knife edge across the beam while monitoring the flux with the QMS placed on the beam axis. This yielded a beam height of 3.2 mm and width of 1.6 mm, giving an area of 0.051 cm^2, or about 10% of the front surface area at normal incidence. Here we have made no allowance for surface diffusion, which is negligible for our conditions. By saturating the Ti getters the pumping speed could be kept constant within 5% for several hours, with a typical value of 600 ℓs^{-1}. The RGA was calibrated with pure N_2 against an ion gauge. Typical fluxes of about 1×10^{16} to 1×10^{15} nitrogen molecules cm^{-2} s^{-1} are obtained for an unchopped beam, with intensities of 100 times lower for a chopped beam. Even the chopped beam intensities are more than a factor of 100 greater than background gas impingment rates with the beam on.

Two different methods were used to determine sticking coefficients. In most cases chemisorption probabilities are determined from the slopes of coverage vs exposure curves. Exposures are controlled by a solenoid-driven flag together, sometimes in conjunction with the 1% chopper operating at 200 Hz. The chopper permits correspondingly longer exposure times for the higher sticking probability measurements, thereby minimizing switching errors. Since the surface atomic density of W(110) is 1.42×10^{15} atoms/cm^2, the beam intensities employed corresponds to ~ 7 to 0.007 monolayer/s of N_2. Surface coverages are estimated by measuring the area under temperature programmed desorption (TPD) peaks using a temperature ramp of 25 K/s. The surface coverage Θ_{N_2} is obtained from temperature programmed desorption (TPD) measurements with a linear heating rate of 25 K/s. Apart from a shift of the TPD spectra by 50 K downward in temperature due to a lower linear heating rate, spectra were essentially identical to those reported in the previous study.[20] These spectra are digitally recorded and stored on disk. The surface coverage is then given by

$$\Theta_{N_2} = \frac{N_T S_{N_2}}{A_b} \int_{t_1}^{t_2} \Delta P_{N_2}(t) dt, \tag{2}$$

where $\Delta P_{N_2}(t)$ is the N_2 partial pressure at time t during the desorption minus any background level and t_1 and t_2 encompass the N_2 desorption peak. Because of the low reactivity of W(110), even with the rate of impingement in the beam at least 100 times higher than from the background pressure, adsorption on other parts of the crystal has to be allowed for. This is done by recording a second TPD spectrum under identical conditions but with the crystal lowered out of the beam path and subtracting the result. This contribution amounts to $\lesssim 20\%$ of the total desorption signal in the worst cases. Before each run the sample was heated to 2400 K to desorb all contaminations. No buildup of carbon could be observed even after extensive heating.

All aspects of this measurement, flag motion, surface temperature variation, signal acquisition, etc. are computer controlled. Notice that determination of beam fluxes and surface coverages [Eqs. (1) and (2)] require the same calibration factors, pumping speed, and beam area measurements. Thus while absolute coverages and fluxes may be accurate to only about a factor of 2, initial sticking coefficients, which depend on the ratio of these quantities, are relatively insensitive to such calibration errors.

For sticking probabilities larger than about 5% a beam reflectivity method is also employed. Agreement between the two methods is always better than a factor of 2, but this reflectivity method is considered to be intrinsically more accurate and is used to calibrate the other approach. This method of measuring sticking probabilities is an adaptation of the method developed by King and Wells,[24] and is based on monitoring of the fraction of the incident beam which is reflected from the surface (i.e., $1 - S$). Here the sample acts as a getter for the incoming beam and the sticking probability is obtained by comparing the pressures vs time with the beam striking the sample to the pressure change when the beam hits a saturated surface with zero sticking probability. In this case the copper wall of the sample mount is used. During several runs the pressure reached an identical final level after a few seconds, so that the assumption of zero sticking coefficient on copper seems to be justified. Exposures to walls and pumps not directly exposed to the beam were always small enough to treat them as constant contribution to the effective pumping speed, therefore the sticking coefficient is given as a function of the pressures P_1 and P_2 with sample in and out of the beam, respectively.

$$S(t) = \frac{P_2(t) - P_1(t)}{P_2(t)}. \tag{3}$$

LEED measurements were made using a 4-grid LEED screen (Varian, 981) which can be observed and photographed through a 15 cm viewport.

III. RESULTS

A. Dependence of initial sticking probability on incidence kinetic energy and angle

The initial sticking coefficient S_0 for dissociative chemisorption of N_2 on W(110) is shown in Fig. 2 as a function of incidence kinetic energy for angles of incidence between 0° and 60°. These data are in good agreement with those reported previously, except that the sticking probabilities are

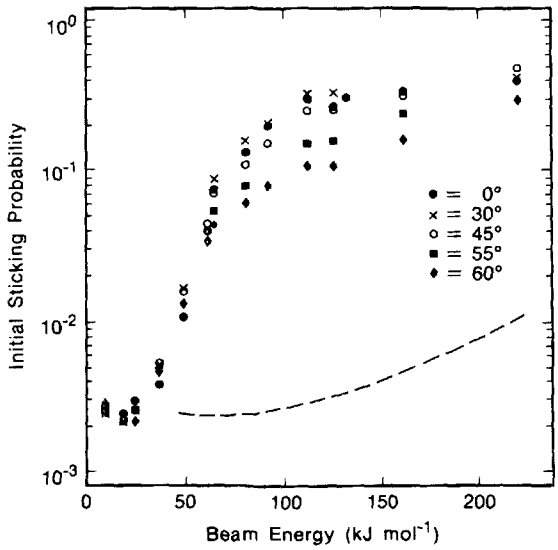

FIG. 2. Initial dissociative chemisorption probability of N_2 on W(110) as a function of the kinetic energy of the incident molecules for angles of incidence between 0° and 60°. Error bars (about ± 25% for the lowest, ± 10% at the highest kinetic energies) are omitted for clarity. The dashed line indicates the predicted behavior for $\theta_i = 60°$, based on normal energy scaling of the 0° data.

somewhat higher here ($\leqslant$ a factor of 2) for the highest energies compared to Refs. 19 and 20, in which no calibration was made against a beam reflectivity method as in the present study. In addition, the energies for the higher energy data points are shifted slightly ($\leqslant$10%) here compared to Ref. 21, due to a revision in the calibration of our ion flight times through the quadrupole. As noted previously, it is seen that the chemisorption probability increases dramatically with incidence energy, rising by more than a factor of 100 for a 100 kJ mol^{-1} increase in E_i. It is seen here, however, that there is relatively little dependence on incidence angle. There is, however, a small but nonnegligible systematic dependence of S_0 on θ_i, a dependence which changes slightly with the kinetic energy of the incident molecules. The data can be grouped into roughly three different ranges of E_i. This is done in Fig. 3 where the initial sticking coefficients relative to $\theta_i = 0°$ are plotted. For $E_i < 30$ kJ mol^{-1} only a slight decrease of S_0 with θ_i is found, which is still within the experimental uncertainties, however. This behavior changes significantly for higher kinetic energies; the sticking probability is a maximum for $\theta_i = 30°$ at $E_i = 48$ kJ mol^{-1}. The decrease at higher θ_i becoming more pronounced with increasing E_i up to 100 kJ mol^{-1}. Notice that this decrease with increasing angle is nearly linear above $E_i = 70$ kJ mol^{-1}. Above 100 kJ mol^{-1} kinetic energy, the relative sticking probability increases slightly with increasing angle, then decreases abruptly in a linear fashion.

In order to test the importance of rotational and vibrational excitations in these experiments, an effusive beam experiment was carried out using a source constructed from a tantalum tube which could be heated to 2000 K. Experiments were performed with this source at 1683 and 1980 K for angles of incidence of 0° and 45°. Pure N_2 effusive beams at these temperatures yielded the sticking probabilities listed in Table I, which are compared with sticking coefficients

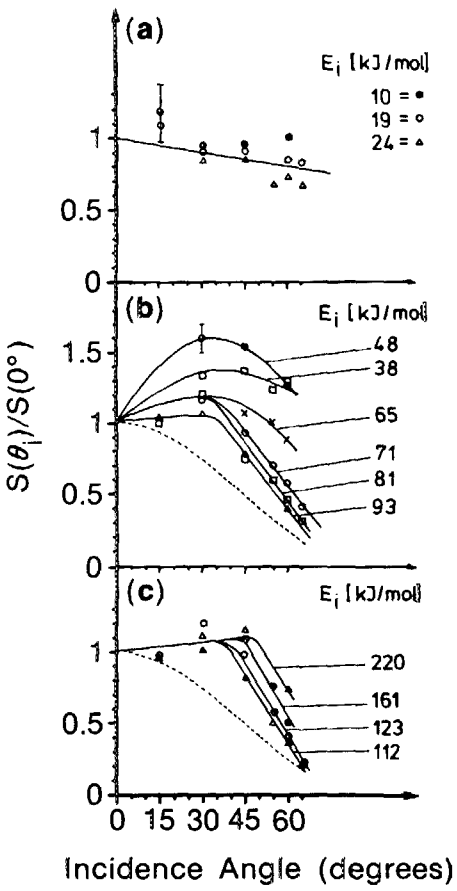

FIG. 3. Relative initial sticking probabilities as a function of angle of incidence for various fixed beam energies. The dashed line indicates normal energy scaling, total energy scaling would give a horizontal line.

predicted by convoluting the above supersonic beam data with a Maxwellian velocity distribution at these temperatures. The energy spread of the supersonic beams is neglected for this purpose, and a linear interpolation between data points shown in Fig. 2 was employed. The difference between the experimental and calculated values are within experimental uncertainties. Since $N_2(v = 1)$ and $(v = 2)$ have populations of ~23% and 6%, respectively, at 1980 K, we conclude that the dissociative chemisorption probability of N_2 on W(110) is insensitive to vibrational excitation or by the extensive population of rotational levels.

B. Angular distribution of scattered N_2

The angular distribution of N_2 scattered from the W(110) surface at an angle of incidence of 45° is shown in

TABLE I. Initial sticking coefficients for effusive beams at various source temperatures.

T_{nozzle}	Angle of incidence	S_0 expt	S_0 calc
1683 K	0°	0.0122	0.0118
1683 K	45°	0.0120	0.0118
1981 K	0°	0.0214	0.0189
1981 K	45°	0.0193	0.0178

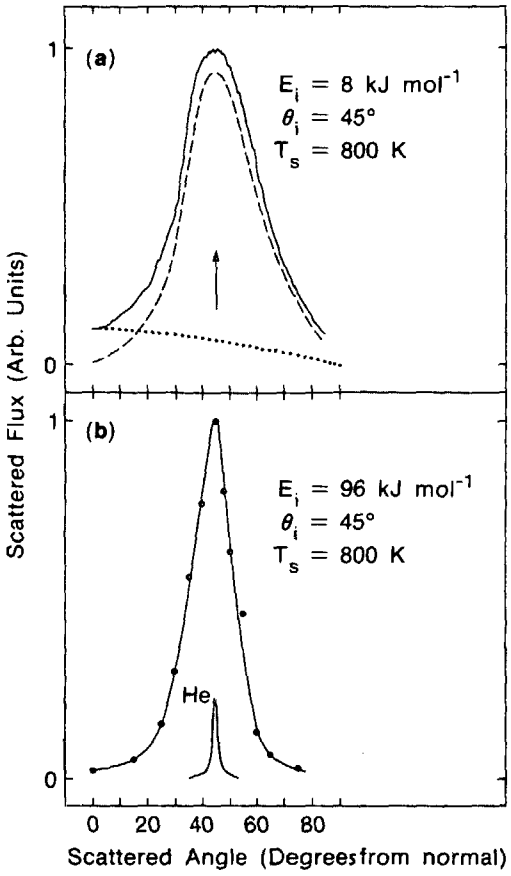

FIG. 4. Angular distribution of N_2 scattering from W(110) at a surface temperature of 800 K for an incidence angle of 45° and with incidence kinetic energy of (a) 8 kJ mol^{-1} and (b) 96 kJ mol^{-1}. Also shown in (b) is a specularly scattered helium beam.

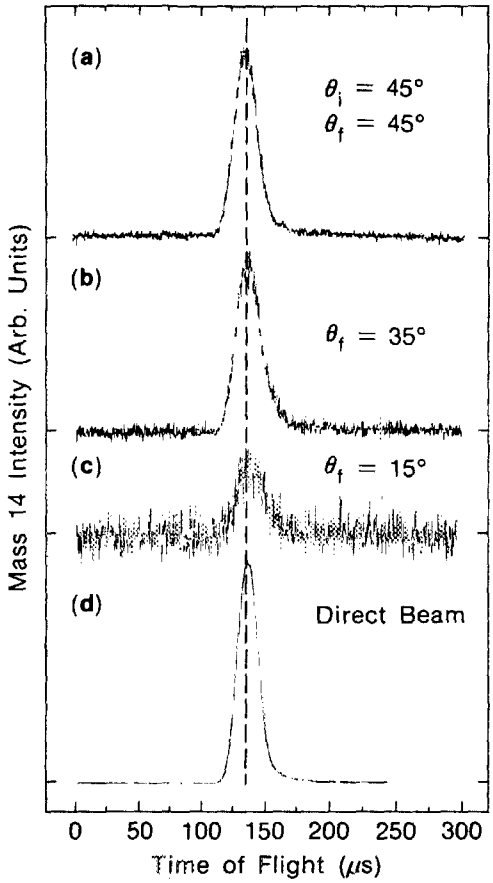

FIG. 5. Typical time-of-arrival distributions recorded at various scattering angles for an incidence angle of 45°, an incidence energy of 96 kJ mol^{-1}, and a surface temperature of 800 K. The chopper function here has a width of ~30 and 10 μs must be subtracted to allow for the flight times of the (mass 14) ions in the QMS. The chopper-to-detector distance was 0.32 m. The dashed line marks the most probable time of arrival of molecules in the direct beam. The scattered peaks all fall close to this line, indicating that the scattering is quite elastic.

Fig. 4 for two kinetic energies and for a surface temperature of 800 K. These data were obtained on the repolished and reoriented surface. The angular distribution of scattered N_2 proved to be sensitive to the surface coverage. Less than 5% of the monolayer of adsorbed N atoms caused perceptible broadening; therefore the coverage was always kept below about 3%. For high energy measurements this was accomplished by working with a chopped beam with 1% duty cycle and recording time-of-arrival spectra for the N_2 signal at each scattering angle. These spectra were accumulated only during the time required for the surface to reach 3% coverage, then the surface was cleaned and three such runs added before integrating the time-of-flight areas to yield the data points such as those shown in Fig. 4(a). Figure 5 displays a selection of the time-of-arrival distributions obtained, as well as that for the direct beam. The chopper pulse width for these measurements was ~30 μs and a delay time of ~14 μs should be subtracted to allow for the ion flight time in the QMS.

The low energy angular distribution displayed in Fig. 4(b) was obtained using a beam chopped with a 50% duty cycle, processing the signal with a lock-in amplifier (PAR, 5101). While the peak of these scattering distributions is always close to specular, the width narrows appreciably with increasing E_i. For the conditions of Fig. 4, we find that at 8 kJ mol^{-1}, the FWHM is ~32° ± 2° and it falls to about 19 ± 1° at 96 kJ mol^{-1}, and to ~15° ± 1° at E_i = 173 kJ mol^{-1}.

These angular distributions were found to be relatively insensitive to surface temperature: an increase of T_s to 2000 K at E_i = 180 kJ mol^{-1} gave exactly the same result as with T_s = 800 K. Finally, the ratio of the maximum of the scattered to the incoming intensity was found to drop from 1.1% at E_i = 115 kJ mol^{-1} to 0.4% at E_i = 185 kJ mol^{-1}. At the same two energies S_0 increases for θ_i = 45° from 0.13 to 0.36, a factor of 3 which corresponds very well to the observed decrease in relative scattered intensity in the specular direction, as explained since dissociative adsorption is competing with this scattering channel.

C. Sticking coefficients as a function of coverage

The sticking probability of N_2 on W(110) was measured as a function of coverage up to coverages of the order of ~0.2 ML for a range of incidence energies. Figures 6 and 7 show examples of the variation in sticking probability with increasing beam exposure for a surface temperature of 800

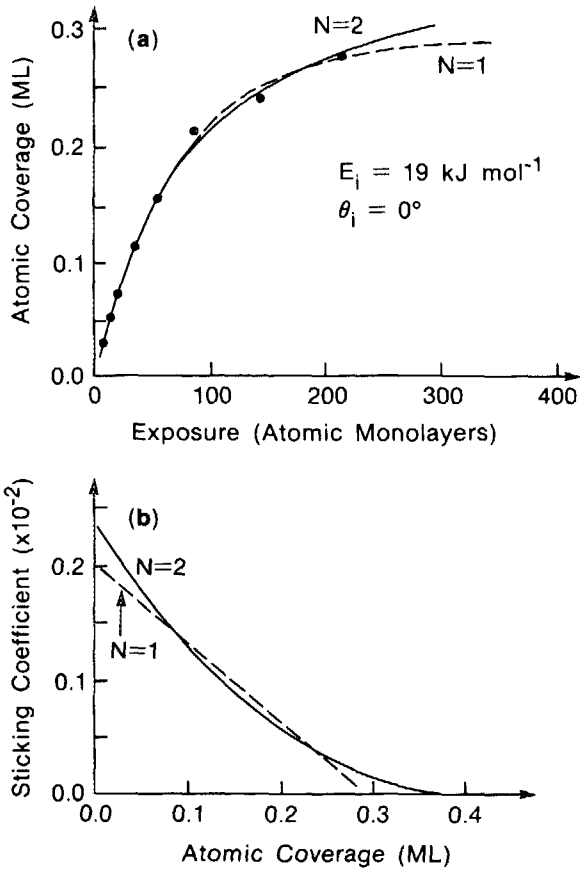

FIG. 6. (a) Surface coverage as a function of beam exposure for N_2 and W(110) for a beam energy of 19 kJ mol^{-1} and an angle of incidence of 0°. Two fitted curves are shown, corresponding to Eq. (4) with $N=2$ (solid line) and $N=1$ (dashed line), see the text. The fit $N=2$ yields $\Theta_{sat}=0.39$ ML and $S_0=0.24\times10^{-2}$. (b) Sticking coefficient as a function of coverage corresponding to these fits. Note that both coverages and exposures are given in terms of atomic monolayers [1 monolayer = 1.41×10^{15} atoms/cm^2 on W(110)].

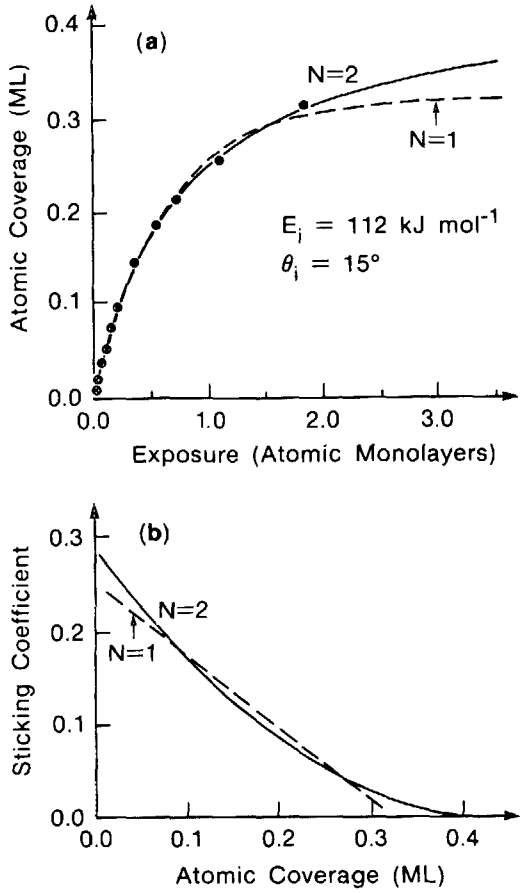

FIG. 7. Same as Fig. 6 but with a beam energy of 112 kJ mol^{-1} and the angle of incidence 15°. Fitting parameters obtained are, for $N=2$, $\Theta_{sat}=0.43$ ML, and $S_0=0.28$ and for $N=1$, $\Theta_{sat}=0.33$ ML, and $S_0=0.25$.

K. Figure 6 shows data for $E_i=19$ kJ mol^{-1} and $\theta_i=15°$, while Fig. 7 corresponds to $E_i=112$ kJ mol^{-1} and $\theta_i=0°$. The chemisorption probability is found to decrease with increasing coverage as reported previously.[20] Our data are consistent with the relation

$$S(\Theta)=S_0(1-\Theta/\Theta_{sat})^N, \tag{4}$$

where Θ_{sat} is a fitting term that corresponds to the saturation coverage for ideal systems, for which $1/\Theta_{sat}$ is equal to the phenomenological number of sites blocked by each adsorbed molecule. For $N=2$, the data of Fig. 6 yield a Θ_{sat} value of 0.38 ML, while that for Fig. 7 gives 0.43 ML. Taking $N=1$ gives 0.29 and 0.33 ML, respectively. While the lower energy data of Fig. 6 is equally well fit by either form, the higher energy results of Fig. 7 give a slightly better fit with $N=2$. In general, the $N=2$ form gives an acceptable fit, over the limited coverage range studied, for all angles of incidence and over the whole range of beam energies. The $N=1$ form also gives a satisfactory fit in most cases, however our previous measurements[21] which were extended to higher coverages actually indicated that an even more rapid fall off than $N=2$ might be appropriate. Beam energies in the range 10 to 100 kJ mol^{-1} yield Θ_{sat} values of $\sim0.35\pm0.05$, for $N=2$ and $\sim0.30\pm05$ for $N=1$. These are somewhat larger than the actual saturation coverage of about 0.25 ML achievable at beam energies of 20 kJ mol^{-1} and less, but smaller than the saturation coverage of about 0.5 ML obtainable with a beam energy of 100 kJ mol^{-1}, indicating deviations of S from Eq. (4) above $\Theta=0.2$, in agreement with the findings of Ref. 20 for $\theta_i=45°$. For higher beam energies Θ_{sat} is continuously increasing as a function of energy up to 0.7 at $E=220$ kJ mol^{-1} but is angle dependent, remaining at a value of 0.35 for $\theta_i=60°$ even at this high energy. As already observed by Somerton and King,[18] the saturation coverage is also a function of T_s at low beam energies. For normal incidence at $E_i=10$ kJ mol^{-1}, Θ_{sat} is reduced by 25% by lowering the surface temperature from 700 to 500 K as measured by Auger. This effect gets smaller with increasing E_i, the difference in Θ_{sat} being less than 10% at $E_i=80$ kJ mol^{-1} for the same difference in T_s.

D. LEED studies

The adsorption of N_2 on W(110) causes the evolution of two well-ordered LEED structures, depending on coverage and surface temperature which can be well correlated with TPD and Auger data. Coverages were determined by mea-

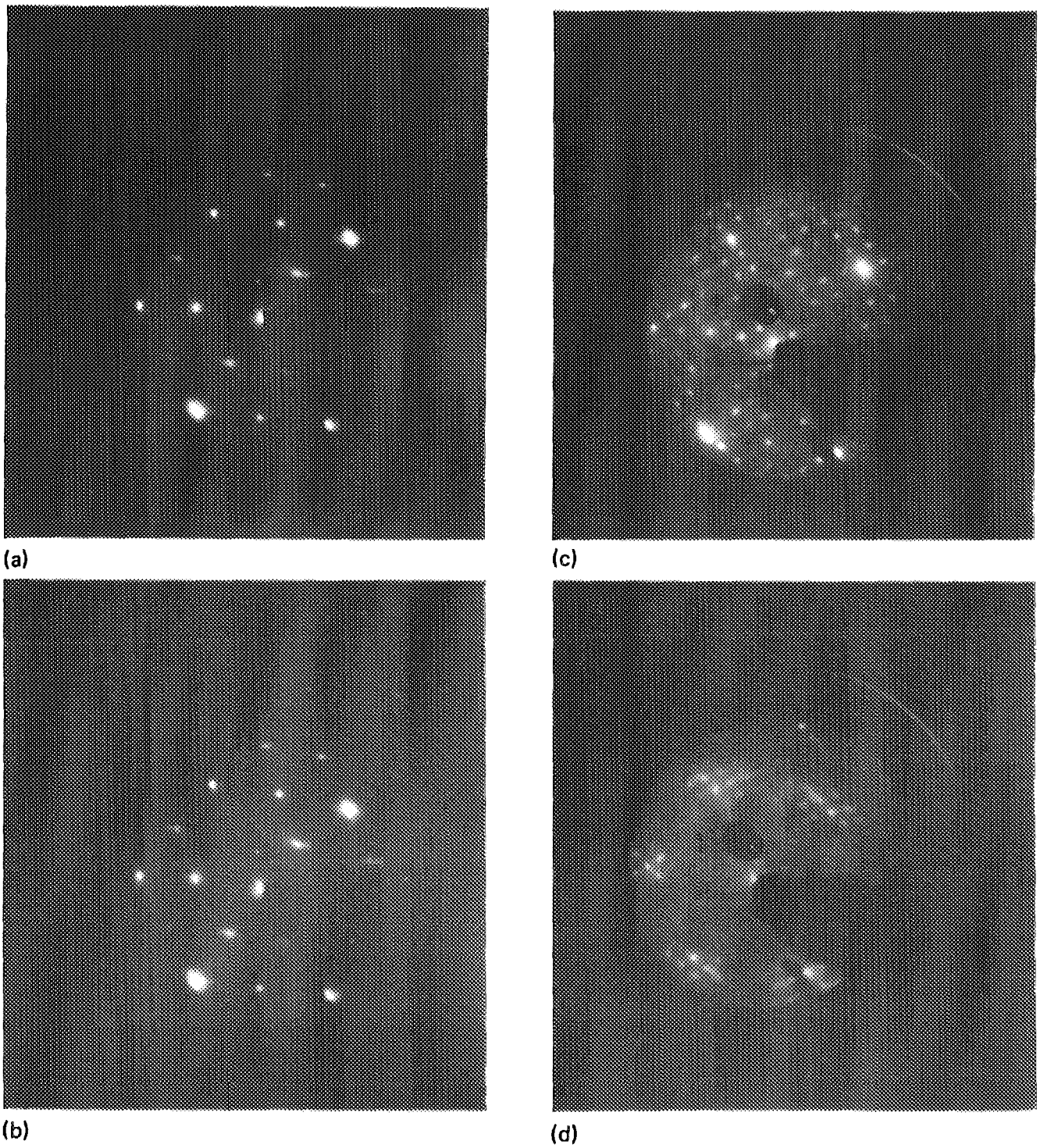

FIG. 8. LEED structures at different coverages: (a) $\Theta = 0.25$ ML; (b) $\Theta = 0.3$ ML; (c) $\Theta = 0.5$ ML; (d) $\Theta = 0.52$ ML.

suring the N(380) eV/W(350) eV Auger peak ratio, assuming a coverage of 0.25 atomic ML for the maximum intensity of the $p(2\times2)$ structure as reported by Somerton and King.[18] Adsorbing nitrogen at 750 K causes the appearance of a faint $p(2\times2)$ structure at coverage as low as 0.1 ML, indicating that ordered islands are formed. This structure becomes visible, however, only at surface temperatures less than 550 K. The intensity and sharpness of the spots increase with decreasing temperature, but the spots remain rather diffuse at this coverage. Increase of coverage results in a sharpening of the superstructure spots, some of them remaining streaky even at a coverage of 0.25 ML [see Fig. 8(a)], probably as a results of the slight misorientation of the crystal. Annealing to 1100 K has no influence on the quality of the diffraction pattern. A further increase of coverage of only 10% completely destroys this superstructure, and only a streaky background with fuzzy $p(2\times2)$ spots remains. The disappearance of the $p(2\times2)$ structure correlates with the appearance of a shoulder in the TPD spectra on the low temperature side of the (single) desorption

peak.[20] Here the coverage is ~0.27 ML which is the maximum coverage that can be achieved with a beam energy of 10 kJ mol^{-1} at $T_s = 750$ K. Coverage can be further increased with higher beam energies,[20] reaching a constant value for kinetic energies above 100 kJ mol^{-1}. A fully developed $c(4\times2)$ structure appears only close to saturation coverage [Fig. 8(c)]. For such complicated superstructures, however, the use of primitive lattice vectors and a matrix notation seems to be more appropriate:

$$\begin{pmatrix} A^* \\ B^* \end{pmatrix} = \begin{pmatrix} 1 & -1/2 \\ 0 & 2 \end{pmatrix} \begin{pmatrix} a^* \\ b^* \end{pmatrix}$$

with a^* and b^* being the reciprocal lattice vectors of the clean surface of the {001} and {$\bar{1}$11} directions. This structure is not well ordered after adsorption at 750 K, but appears after annealing at 950 K even at that temperature. From Auger peak ratios, a coverage of 0.5 atomic ML was determined for the $c(4\times2)$ structure. This corresponds to the fully developed β_2 peak in the TPD spectra.[20] At intermediate coverages, a fuzzy mixture of $p(2\times2)$ and parts of a $c(4\times2)$ structure is visible [Fig. 8(b)]. An increase of coverage beyond 0.5 up to saturation at about 0.52, correlating with the β_1 peak,[20] makes the $c(4\times2)$ structure fuzzy again [Fig. 8(d)].

IV. DISCUSSION

The following discussion is divided into five sections dealing with various aspects of the above results. Section IV A concerns the normal incidence data. Here we have analyzed the variation of the sticking probability with kinetic energy in terms of a barrier height distribution for chemisorption and have extracted a form for this distribution consistent with our results. We also contend that N_2 chemisorbs on the perfect W(110) surface even at low energies. In Sec. IV B, we consider possible models to account for the observed breakdown in normal energy scaling. We show that our results can be explained by two types of model: those which invoke a corrugated surface and those that involve multiple encounters between the molecule and the surface. In the former case, we speculate that the corrugation could be associated with an N_2 species that has already interacted chemically with the surface. The latter case may also involve an intermediate species that interacts chemically with the surface. Thus we believe that the breakdown in normal energy scaling implies that the molecule passes through a intermediate state which is a "dynamical precursor" to dissociation. Section IV C considers the observed angular distributions. Unfortunately these are found to be of only limited value in helping to understand the chemisorption dynamics. We observe predominantly direct-inelastic scattering, but because of the experimental insensitivity to molecules scattered diffusely, we cannot rule out a substantial cosine component. Sections IV D and IV E deal with the sticking vs coverage and LEED data which illuminate the process of chemisorption on partially covered surfaces.

A. Dependence of initial sticking probability on kinetic energy for normal incidence

Clearly, the initial dissociative chemisorption probability of N_2 on W(110) increases dramatically with increasing translational energy. This is consistent with the presence of a potential barrier to dissociation. It is seen from Fig. 2 that after a nearly constant value at low kinetic energies, S_0 begins to increase at around 40 kJ mol^{-1}, rising by more than a factor of 100 before leveling off for $E_i > 100$ kJ mol^{-1}. The value of $S_0 \approx 2.5\times10^{-3}$ for $E_i \leqslant 30$ kJ mol^{-1} is in good agreement with the value of 0.003 ± 0.001 for N_2 gas at 300 K reported in the literature.[16–18] At the highest energy of 220 kJ mol^{-1}, a sticking probability of 40% is reached, and the S_0 values appear to continue to increase slightly with increasing E_i.

Although the dynamics of dissociation may be very different than for the present case, this observation of strong translation activation is qualitatively similar to that observed previously for the dissociative chemisorption of CH_4[5] and O_2[6] on this same surface, and to the behavior reported for the H_2/Cu system,[2–4] and to that observed recently for CO_2 on Ni(100).[7] The initial sticking probability of CH_4 on this surface is found to increase even more dramatically than the results reported here, with S_0 rising by a factor of over 10^4 for a 100 kJ mol^{-1} increase in E_i. In this case, we have proposed that much of the dramatic increase results from a quantum tunneling process, whereby hydrogen tunnels through the activation barrier at energies below the classical barrier height. This mechanism is almost certainly negligible for N_2 dissociation. For methane, S_0 increases continuously up to the highest energies reached, attaining a value of about 10% at about 100 kJ mol^{-1},[5] while in the case of O_2, we find a fairly sharp rise from about 10% at 10 kJ mol^{-1} to essentially unity at about 40 kJ mol^{-1}.[5] The sticking probability for H_2 is found to reach about 14% on the Cu(110) surface at ~34 kJ mol^{-1} and about 10% on the Cu(100) surface at this energy.[2–4] Dissociation of CO_2 on Ni(100) increases from a probability of 5×10^{-4} at 8 kJ mol^{-1} to 0.15 at 100 kJ mol^{-1}.[7]

In contrast to these highly activated systems, where overcoming the activation barrier is the rate-limiting step, the sticking probability is found to fall with increasing energy in the case of the molecular chemisorption of CO on Ni(111)[25] and Ni(100).[26] For these systems, the initial sticking probability is close to unity at energies of $\leqslant 5$ kJ mol^{-1}, falling by about a factor of 2 by about 50 kJ mol^{-1}. Although there is currently disagreement as to the existence of an equilibrated intrinsic precursor to chemisorption on these surfaces, CO appears to reach the chemisorption state only after first trapping in a relatively weak physisorption well. Increasing translational energy may then prevent this initial trapping. It seems likely that such a process does not make an important contribution to the present observations for the N_2/W(110) system.

The general shape of the N_2/W(110) curve shown in Fig. 2 is qualitatively similar to that reported for the H_2/Cu system,[2–4] although in that case only a factor of ~5 overall increase in S_0 was observed with increasing E_i, and normal energy scaling was reported. In both cases an S-shaped curve

is observed, with the increase in S_0 occurring over a fairly wide range of E_i. This is contrary to what would be expected from a single barrier to chemisorption and has been explained in the case of H_2/Cu system in terms of there being a distribution of barrier heights. The increase in S_0 with E_i for N_2 on W(110) is seen to extend over more than 50 kJ mol^{-1}. If we apply this same interpretation, our data suggest a fairly wide distribution of barrier heights. In this picture, the S_0 values are taken as being proportional to the fraction of the barriers surmountable at energy E_i, and the slope of the S_0 vs E_i curve is proportional to the relative probability of finding a barrier of height E_i. Figure 9 displays a Gaussian barrier height distribution that has been fitted to the 0° data using a nonlinear least squares fitting routine, where the Gaussian shape is imposed as a constraint to the fit, according to

$$S_0(E_i) = \eta(E_i,E) \int_0^{E_i} \exp\left[\frac{-(E_i - E_0)^2}{\sigma^2}\right] dE, \quad (5)$$

where $\eta(E_i,E)$ is an efficiency factor equal to the probability of dissociation for a molecule with incidence energy E_i encountering a barrier of height E.[2] Here the finite energy spread of the beam is neglected, being a factor of 10 or so narrower than the barrier height distribution, and $\eta(E_i,E)$ is taken as a constant. This approach is equivalent to differentiating a smooth curve fitted to the data points and gives the same result. We obtain a best fit with $E_0 = 92$ kJ mol^{-1} and $\sigma = 36$ kJ mol^{-1}, and $\eta(E_i,E) = 0.36$. Our fit assumes that all of E_i is available to overcoming the barrier. If only a fraction of E_i is actually accessible to the reaction coordinate, this energy scale will be correspondingly compressed. The origin of this barrier height distribution is a key question and intimately tied to any model of the dynamics of the dissociation process. It is possible that such a distribution arises due to variations in the barrier height with the orientation angle of the internuclear axis, the impact site in the surface, the vibrational phase of the incident molecule, or some combination of these factors. Since we observe approximate total energy scaling in this system, it should be noted that a similar distribution of barrier heights will apply to nonnormal incidence.

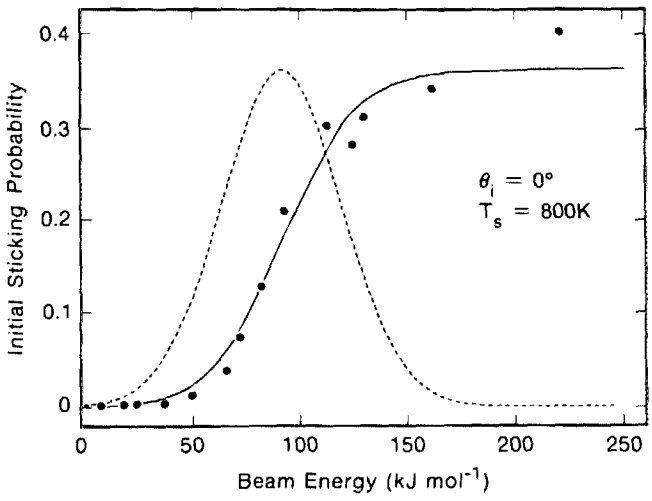

FIG. 9. Initial sticking probability of N_2 on W(110) as a function of incidence kinetic energy for normal incidence. The dashed curve represents a Gaussian barrier height distribution corresponding to the relative probability of a molecule dissociating at a given incidence energy. This has been fitted to the sticking probability data with the Gaussian shape imposed as a constraint to the fit, as described in the text.

The value of E_0 obtained here (92 kJ mol^{-1}), is considerably higher than the barrier heights of 17.4 kJ mol^{-1} extracted by Cosser *et al.*, from angular resolved TPD measurements.[15] Considering microscopic reversibility, one might expected closer agreement between these values. We will return to this discrepancy in the next section.

Figure 2 shows that S_0 is fairly constant at about 0.002 ± 0.001 for $E_i \leqslant 40$ kJ mol^{-1}. It is tempting to attribute this residual probability to dissociation at surface defects. This contention is supported by the observations of Besocke and Wagner[27] who examined the adsorption of N_2 on W(110) vicinals for ambient gas (energies of $\leqslant 10$ kJ mol^{-1}) and reported that dissociative chemisorption occurs at step sites, which are continuously vacated by surface migration. Similarly, Singh-Boparai *et al.*[28] examined the chemisorption of N_2 on a number of tungsten faces and concluded that dissociation takes place only on vacant pairs of {100} sites. A somewhat similar conclusion had been reached earlier by Adams and Germer, who compared the dissociative chemisorption probabilities for N_2 on a number of tungsten faces,[29] and reported that chemisorption only occurs with a high probability on geometric sites characteristic of the {100} plane. However, we have found no significant difference in the sticking coefficient at low E_i (within $\pm 25\%$) on surfaces cut at $0.0° \pm 0.5°$ and $1.5° \pm 0.5°$ from the true W(110) plane. Here the steps on the misoriented surface are oriented almost parallel to the {110} direction (as determined by LEED). Such steps are expected to be less reactive than steps along the {001} direction,[27] but S_0 should still differ by more than a factor of 5–10 for these surfaces if a linear extrapolation is appropriate. Further, the good agreement between our low energy measurements and previous studies[16–18] suggest that the dissociative chemisorption probability of N_2 may be of the order of a few parts in a thousand, even on a perfect W(110) surface. This is consistent with the field emission tip measurements of Polizzotti and Ehrlich,[30] who concluded that N_2, unlike H_2, does chemisorb on the perfect W(110) surface.

B. Dependence of initial sticking probability on angle of incidence

It is clear from Figs. 2 and 3 that the dissociative chemisorption probability is relatively insensitive to incidence angle. Such behavior is contrary to what would be expected from a 1DB model, as discussed in the introduction. This is emphasized in Fig. 2 where the dashed line represents the energy dependence for the case of 60° incidence calculated from the normal incidence data assuming that this system follows normal energy scaling, so that $E_n = E_i \cos^2 \theta_i$. Clearly the data scale more closely with the total incidence kinetic energy. This is a rather surprising result, since activated dissociative chemisorption of both CH_4[5] and O_2[6] on this surface exhibit normal energy scaling, as does the H_2/Cu[2–4] and CO_2/Ni[7] systems.

Total energy scaling implies that the parallel momen-

tum of the incident molecules is equally efficacious in overcoming the potential barrier to chemisorption as is normal momentum. Access of parallel momentum on a single collision would require a substantially corrugated gas–surface potential. Alternatively, if the incident molecule is temporarily trapped in a precursor-like state, relatively low levels of corrugation would be sufficient to couple to the initial motion parallel to the surface. We will explore these two possibilities in turn.

1. Corrugated surface model

The {110} plane is the most densely packed tungsten surface and would be expected to be fairly flat in the thermal energy scattering regime. Thus helium scattering at ~ 6 kJ mol^{-1} is dominated by a single specular peak (see Fig. 4). However, the increase in S_0 does not occur until incident energies of $\geqslant 40$ kJ mol^{-1}, at which point the molecules could conceivably penetrate the surface sufficiently to experience the corrugation in the interaction potential associated with the individual surface atoms. This would correspond to the "structure scattering" regime as defined by Oman,[31] who described a transition from "thermal" to "structure" scattering arising from an increased apparent surface roughness caused by deeper penetration into the repulsive potential field of the surface at higher incident energies. The insensitivity of S_0 to incidence angle would then arise because the N_2 molecule penetrates the surface to a point where the quasi-spherical nature of the individual tungsten atoms is probed. Measurements[32–34] and calculations[31] of argon and neon scattering from Ag(111) suggest that the degree of penetration at ~ 40 kJ mol^{-1} would be relatively slight. For example at this normal kinetic energy the widths of the angular scattering distributions for neon and argon on Ag(111) are found to be less than 20°.[34] Similarly, in a study of the scattering of argon from Pt(111), Hurst *et al.*[35] saw no direct evidence of structural scattering for energies up to 165 kJ mol^{-1}, although an increase coupling between the gas and surface atoms was indicated by an observed twofold increase in the sensitivity of the scattered velocity distributions to surface temperature in going from ~ 6 to ~ 165 kJ mol^{-1}. That there is a similar lack of penetration is supported for the N_2/W(110) system by the observed angular distributions (see Fig. 4). The angular distributions for 45° incidence continue to become narrower up to the highest energy examined of 173 kJ mol^{-1}. The degree of penetration necessary to yield the observed total energy scaling in a *direct* process would almost certainly lead to considerably broader angular distributions.

A high degree of corrugation could be experienced in the absence of deep penetration if the molecules interact *chemically* with the substrate prior to overcoming the activation barrier. Such a chemical interaction might indeed be highly corrugated, as evidenced by the fact that different binding sites may have substantially different energies, and here the interaction potential may vary strongly over the surface. This possibility is supported by the fact that nitrogen is known to absorb molecularly on this surface,[36–38] into the N_2-γ state which has an adsorption energy of about 30 kJ mol^{-1}, as measured by thermal desorption.[37] On other tungsten surfaces a second molecular state, the α state, is also observed, with an even stronger binding energy of ~ 50 kJ mol^{-1}.[36] While the α state has not been observed for the W(110) surface, this may simply be because dissociation occurs after a time short compared to observation times. This state may nevertheless be encountered by all approaching molecules. Menzel and co-workers[38,39] have carried out SCF-$X\alpha$ scattered wave calculations for N_2 on Ni clusters and have modeled photoemission data for the γ-N_2 on W(110). Their results suggest a strong chemical interaction in all cases, with the $N_2 5\sigma$ orbital being pulled down close to or below the 1π orbital. They also find that this interaction is highly localized, with the chemisorption bond being confined to a single metal atom.[39] This contrasts with the results of similar calculations for CO which reveal that the bonding orbitals extend as far as the third neighbor atoms.[39] Such highly localized bonding for N_2 would result in a corrugated surface potential and may indeed account for the observed total energy scaling.

Without detailed calculations, it is difficult to expand further on this idea, however, it should be pointed out that the presence of a bound state does not necessarily lead to total energy scaling, since methane is also known to adsorb molecularly to W(110) with a binding energy of ~ 30 kJ mol^{-1},[40] very similar to that for γ-N_2. It may be that for this case the interaction is delocalized, giving a rather flat surface potential.

2. Multiple encounter model

The observed behavior can be accounted for in the absence of a high degree of surface corrugation if we propose that dissociation occurs at least partially via an intermediate state, such that the molecule undergoes sufficient collisions with the surface to effectively scramble parallel and perpendicular (normal) momentum components. Gadzuk and Holloway[41] have suggested that the intermediate state concerned in this process could be a N_2^- negative ion species and have discussed our results in this light. In their picture, the affinity level of the N_2 falls below the Fermi level at some critical distance, from which point inward an electron can tunnel (harpoon) onto the incoming molecules to form a negative ion.[41,42] They postulate that the N_2^- species would be formed without requiring appreciable activation. Dissociation occurs from within the negative ion state, but requires activation (barrier in the exit channel). The total energy scaling then occurs as the energy associated with the motion parallel to the surface is coupled into intramolecular vibrational energy, which is in turn mixed with the normal kinetic energy by nonlinear coupling forces. Note that to account for the observed total energy scaling, this model requires that the coupling to parallel momentum must be fast enough to allow dissociation to occur before the translational energy is dissipated to phonons. Here the underlying crystal structure or surface imperfections mediate the transfer of energy between parallel translational and vibrational motions, so that the potential surface for the intermediate has substantially increased corrugation.

The curve-crossing distance for formation of an N_2^- species can be estimated from knowledge of the work function

of W(110) and the electron affinity of N_2.[40,41] Taking values of 5.5[43] and -1.9 eV[44] for these, respectively, we estimate a crossing distance of 0.5 Å from the image plane. It is questionable whether the molecule could approach so closely without activation. However the essence of this picture is by no means confined to ionic intermediates. Clearly the N_2-γ and α states could also act as intermediates. The net charge associated with the molecule is unknown for these states, but cluster calculations[39,45] suggest that the net charge on the nitrogen is unlikely to be as much as a full electron, being much closed to a neutral species. However, the dynamical role of this intermediate, causing parallel and perpendicular momenta to be mixed, is not particularly dependent on its net charge. Finally we note that the potential experienced by a charged species might well be signifcantly corrugated due to the exclusion of the image charge from regions close to the atomic nuclei, so that a negative ion species is also a candidate for the above "chemical corrugation" model.

Thus we find that the observed breakdown in normal energy scaling can be rationalized only by assuming that the incoming molecule interacts strongly with the surface prior to the dissipation of its kinetic energy. The molecule can be thought of as passing through an intermediate chemical state distinct from the free N_2 molecule. This state is then a precursor to chemisorption. It is important to distinguish the dynamical role of this state from the kinetic role of the classical precursor state. This precursor may not be equilibrated, but may be closer to a transition state than to a long-lived intermediate. The sticking vs coverage data discussed in Sec. IV D below in no way resembles that expected for a classical precursor.

The foregoing discussion is based on the idea that the incidence kinetic energy serves to overcome a barrier to dissociation. To account for the observed total energy scaling in this case requires a model in which the parallel translational energy does work against forces operating parallel to the surface, and we have speculated on the possible origin of such forces. Alternatively, it is possible that the observed translational energy dependence stems rather from a velocity-sensitive process. Thus the approach velocity might effect the sticking coefficient by changing the transition probability between two adiabatic potential surfaces in the region of an avoided crossing of two diabatic curves.[40,41,46,47] For example, if dissociation occurred only via the upper of two diabatic surfaces, it would be necessary for the system to undergo a diabatic transition in order for chemisorption to take place. In this case, the observed insensitivity to incidence angle would imply that the separation between the two adiabatic surfaces is a strong function of position in the surface plane, as well as along the surface normal. Thus if the crossing region is highly localized in all directions, both parallel and normal components of the approach velocity may influence the transition probability and hence the sticking coefficient. In fact, such processes can be regarded as being due to generalized static and dynamic "surface corrugation."

3. Microscopic reversibility

The insensitivity of the chemisorption probability to incidence angle is in conflict with the measurements of Cosser *et al.*[15] who reported that the angular distribution for molecules desorbing from the covered surface is strongly peaked along the surface normal. Detailed balance arguments associated with microscopic reversibility predict that chemisorption would be substantially enhanced for normal incidence, with normal energy scaling for example. The data of Fig. 2 can be used to synthesize an angular distribution for molecules desorbing from a 1500 K surface. Assuming a Boltzmann distribution of velocities at the surface temperature and following the method described in by Cardillo *et al.*,[4] we obtain a roughly cosine angular distribution of desorption angles, in contrast to the $\cos^4\theta$ dependence reported by Cosser *et al.*[15] In addition, as mentioned above, the barrier height extracted by us is considerably higher than that extracted from these desorption measurements. We may account for these apparent discrepancies in several ways: first, detailed balancing rigorously requires that exactly the same quantum states be considered in both directions. This does not apply here where we have no knowledge of the quantum state distribution of the desorbing molecules. The desorbing molecules *could* all be in vibrationally excited states for example, which are absent from the incident beam. The rotational and vibrational temperatures of supersonic beams are much lower than the desorption surface temperature. Because of the highly nonequilibrium nature of these two experiments, results must be expected to be dominated by dynamics rather than by thermodynamics, and therefore the lack of agreement may not be so surprising. Further, the desorption data refer to desorption from a saturated surface, whereas Fig. 2 refers to chemisorption on the clean surface. Finally we note that the range of energies covered by a Boltzmann gas from a 1500 K source largely corresponds to the low-energy-limit data, the dynamical origin of which is by no means clear.

The fact that the angular distribution of desorbing molecules peaks in the direction of the surface normal does not necessarily indicate the existence of a one-dimensional barrier in front of the surface. In recent angular resolved TPD measurements of H_2 desorbing from Ni(111) and Ni(110), Steinrück *et al.*[13] have observed peaked angular distributions, with a $\cos^{4.6}\theta$ dependence, even though they believe there to be no barrier to chemisorption for these systems. To the extent that the measurements of Cosser *et al.*[15] refer to the nonactivated region of the N_2/W(110) data, these observations may be viewed as similar. Comsa and co-workers have examined the angular and velocity distributions of D_2 molecules desorbing from Cu(100), Cu(111), and Ni(111) surfaces following permeation through the bulk.[10] They find that while the angular distributions are fully consistent with the 1DB picture, the velocity distributions cannot be accounted for by such a model. The mean velocity of the desorbing molecules is observed to be essentially independent of desorption angle, at least out to $\sim 60°$ from the normal, whereas a 1DB model would predict a rapid increase in velocity with increasing angle from the normal. It is possible that a mechanism based on an intermediate which causes mixing of parallel and perpendicular momenta, may also apply to this case. Thorman and Bernasek,[11] in post-permeation desorption experiments on the N_2/Fe(111) system, and

more recently Kubiak *et al.*,[12] in measurements on the hydrogen/Cu(110) and Cu(111) systems, have both observed populations of vibrationally excited molecules in excess of what would be expected for a Boltzmann distribution at the surface temperature. Such behavior is also not accounted for by a simple 1DB model. Kubiak *et al.* have further shown that the existing data for chemisorption and post-permeation desorption of hydrogen and copper surfaces are inconsistent with the principles of detailed balance. This is contrary to earlier work of Cardillo *et al.*[4] which showed that the angular distributions of hydrogen desorbing from Cu(100) and Cu(110) *can* be successfully synthesized from the energy and angular dependence of the dissociative chemisorption probability using detailed balance analysis.

C. Angular distributions

The angular distributions of N_2 scattered from W(110) are found to peak close to the specular direction and to become narrower with increasing incidence energy. Similar distributions have been observed for Ar scattering from various surfaces[31–34] and for N_2 scattering from Ag(001),[48] Ag(111),[49] and Pt(111),[50] where this same trend is found. For example, while we find widths (FWHM) of $32° \pm 2°$ and $19° \pm 1°$ for $E_i = 8$ and 96 kJ mol^{-1} for $\theta_i = 45°$ and $T_s = 800$ K, widths of 30° and 10° are observed for scattering from Ag(001) for $E_i = 7$ and 96 kJ mol^{-1}, respectively, for $\theta_i = 60°$ and $T_s = 300$ K.[48] The slightly narrower distributions in the latter case are to be expected due to the lower surface temperature and large incidence angle employed. As with the present data, all distributions are found to peak very close to specular.[48] In another study,[49] Asada reported a width of $\sim 37° \pm 3°$ for $E_i \sim 3$ kJ mol^{-1} for an effusive N_2 beam scattering from Ag(111), with $\theta_i = 45°$ and $T_s = 500$ K. Such quasispecular distributions are attributed to direct-inelastic scattering, in which the molecule makes only one or two collisions with the surface.[51]

In Sec. IV B above, it was suggested that the observed insensitivity of S_0 to θ_i arises due to an intermediate state which is either the source of "chemical corrugation" or mediates the scrambling of parallel and perpendicular velocity (energy) components. Such processes would also be expected to dramatically broaden the scattering distribution. In the latter case a cosine distribution peaked along the surface normal would be expected, while the degree of corrugation necessary to account for total energy scaling might be expected to lead to diffuse but somewhat sharper scattering. At first sight the data of Fig. 4 appear to go against this view. However, the models can be reconciled with these data if certain additional assumptions are made. We must assume for example that only a fraction of the incident molecules can enter the intermediate state, say those within a given range of orientation angles. The remainder then give rise to the predominant features of the in-plane angular distributions reported above. Since we have proposed that the barrier to chemisorption is between this intermediate state and the product states, those molecules that fail to surmount the barrier must leave the surface and should contribute to a diffuse scattering component. The dashed curve in Fig. 4(a) indicates a possible contribution due to such a process. For this case, $S_0 \sim 0$, so that essentially all molecules are scattered. Allowing for the differing solid angles into which the direct and cosine components are scattered indicates that the diffuse component may account for as much as 70% of the scattered intensity, with 30% scattering directly. Here we have assumed that the direct inelastic peak has an out-of-plane width of 40% of the in-plane width, as observed by Asada.[49] Similarly, we estimate that the narrow angular distributions recorded at $E_i = 96$ kJ mol^{-1} would display a peak intensity of ~ 70 times that for an equivalent flux distributed over 2π. Allowing for the same 70:30 branching between channels and for the molecules which stick (which are lost from the diffuse channel) we predict a diffuse intensity along the normal of about 2% of the intensity at the peak of the direct inelastic peak. Such a signal would be at the limit of our sensitivity. Moreover, this contribution may be considerably more spread out, and even delayed in time, making detection even less likely.

An additional constraint to the modeling of the dissociation dynamics is the observation that the intensity of scattered molecules associated with the direct-inelastic peaks is found to fall by about a factor of 2 as E_i is raised from 100 to 200 kJ mol^{-1}. This is in good agreement with the observed fall in S_0, indicating that, over this energy range at least, the effective barrier to dissociation is prior to the intermediate state. The full quantification of the diffuse scattering intensity as a function of incidence energy would clearly be a sensitive test of the proposed model and should be examined further.

D. Variation of sticking probability with surface coverage

The sticking probability of N_2 on W(110) is found to fall off with coverage roughly according to Eq. (4) with $N = 1$ or 2, at least up to coverages of ~ 0.2 atomic ML, in agreement with our previous reports.[20] This behavior is qualitatively similar to that observed for N_2 chemisorption on the {111} and {411} faces of tungsten but contrary to that reported for the {320}, {310}, and {100} surfaces.[17,28,52] For these latter three faces, the chemisorption probability is probably not dominated by an activation barrier. It is found to remain fairly constant up to ~ 0.25 atomic ML. This behavior has been interpreted in terms a precursor model in which the trapping probability in an (extrinsic) precursor state is roughly independent of whether the molecule strikes a filled or vacant site. For the present case, and for the {111} and {411} faces, the sticking probability clearly *does* depend on the occupancy of the "target" site. A precursor mechanism is not ruled out by such behavior, since for example, trapping into the (intrinsic) precursor state could be possible only at an empty site. As has been shown by Kisliuk,[53] and more recently by Yoshimori and Odoi,[54] precursor-based models can yield almost any form of sticking vs coverage curve, depending on such things as the evaporation rate out of the state, the mobility of the precursor and the degree of long- and short-range order. However, as discussed above we believe that chemisorption of N_2 on W(110) may proceed via a molecular intermediate, or "hot" precursor, that is quite different in its dynamical role from the classical picture

of a precursor to chemisorption. Evidence for such a state was recently presented for the CO/Ni(100) system.[25]

The LEED observations indicate that island formation occurs at coverages of about 0.1 atomic ML. If island formation were perfect and the sticking probability on an ordered $p(2\times2)$ surface were negligible, we would predict $N=1$ in Eq. (4), with $\Theta_{sat}=0.25$ ML at low energies. This is not inconsistent with the present observations, but *is* contrary to previous findings.[20] The data shown in Fig. 6, taken with $T_s=800$ K, $E_i=20$ kJ mol^{-1} and $\theta_i=0°$, can be fit quite well by Eq. (4) with $N=1$, yielding $\Theta_{sat}=0.29$ ML. This compares with $\Theta_{sat}=0.38$ ML for a fit with $N=2$. The accuracy of these two fits are comparable and not distinguishable within the experimental uncertainties. Previous measurements,[20] which are extended to higher coverages were found to be consistent with $N=2$. The higher energy data of Fig. 7 were also seen to give a marginally better fit with the $N=2$ form, contrary to the predictions of a simple island-formation picture. It seems likely that the "true" value of N is between 1 and 2, and that both island formation and site-exclusion factors play a role. As was mentioned above, the saturation coverages obtained as fits to the 0 to $\sim$0.2 ML coverage data, are found to be somewhat higher than the true saturation coverages, indicating deviations from Eq. (4) at higher coverages.

The observation that the saturation coverage can be increased by raising the incidence energy suggests that the number of sites available for chemisorption is energy dependent, as is evidenced by the increase in S_0 with E_i. At energies of 5 kJ mol^{-1} or so, $\sim$0.25 atomic ML is sufficient to reduce the sticking probability to close to zero. At this point sticking can be reactivated by increasing E_i, reaching a sticking probability of $\sim 10\%$ for $E_i=100$ kJ mol^{-1}. Obviously the effective barrier height increases with surface coverage in this system. If the sticking vs coverage data is interpreted in terms of available sites for chemisorption, having different barrier heights, the geometric constraints are clearly reduced with increasing incidence energy.

E. LEED structures

As stated above, a coverage of 0.25 ML is sufficient to reduce the sticking probability to close to zero for molecules striking the surface with only a few kJ mol^{-1} kinetic energy. This surface coverage is associated with the $p(2\times2)$ LEED structure given in Fig. 8(a). This structure is in agreement with that reported by Somerton and King[18] and indeed reaches a peak intensity at the (low-energy) saturation coverage of 0.25 ML. From the combined evidence of variable incidence angle Auger electron spectroscopy and ion scattering spectroscopy, Somerton and King have proposed that the N atoms do not occupy conventional overlayer sites at this coverage, but are sandwiched between the top two layers of tungsten atoms. A useful guide to possible underlayer structures can be obtained by considering the known structures of the bulk tungsten nitrides.[55] A wide range of stoichiometries have been recorded for these compounds which form fcc, simple cubic, hexagonal, and orthorhombic phases.[55] They all have in common a tungsten nearest neighbor (NN) distance that is about 5% wider than in the pure W bcc lattice. It should therefore not be surprising that the W surface reconstructs when saturated with dissociated nitrogen atoms in order to achieve configurations more similar to those found in tungsten nitrides. Since this behavior has not been reported for any other tungsten surface, the distinguishing feature of the {110} surface may be its high surface-atom density, being the most densely packed tungsten face. Looked at another way, with a coverage of 0.25 ML, one might expect a structure similar to bulk W_2N, the surface

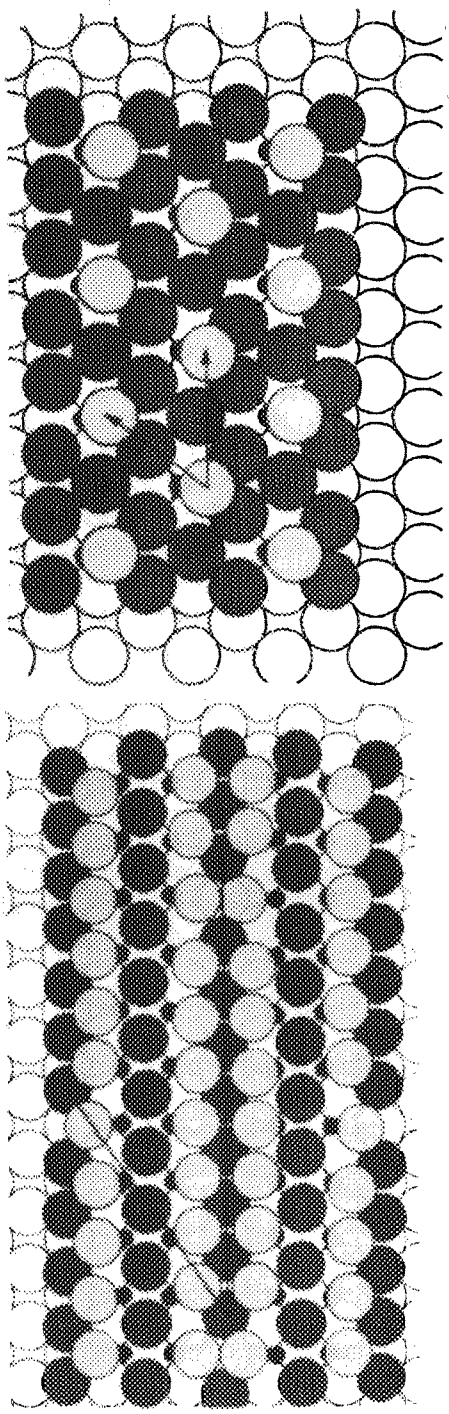

FIG. 10. Schematic models of possible structures for nitrogen on W(110) at coverages of 0.25 (a) and 0.5 (b). In both cases the nitrogen atoms are drawn as black dots, the W atoms of the first layer are heavily shaded and the lightly shaded atoms have moved out of the original plane. The unshaded ones are in the second layer.

being a cut through a plane of nitrogen atoms. W_2N forms fcc, hexagonal and orthorhombic phases,[55] and, for example, in the fcc phase the N atoms are always located at interstitial sites of a W fcc lattice which has a lattice constant of 2.91 Å, compared to 2.74 Å in the pure metal. Interstitial sites similar to the (1/4, 1/4, 1/4) site in bulk W_2N exist on the W(100) but not on a W(110) surface. N atoms are therefore more favorably accommodated in the {110} case by penetration into the first layer. It is possible that this difference in available surface sites is related to or even accounts for the differences in reactivities of these two surfaces. Because of the mismatch of lattice constants, a widening up of the W lattice is favored in the close packed directions. This is achieved by the raising of some of the W atoms slightly out of the close packed rows. Such shifts of W atoms are energetically unfavorable with respect to the pure W lattice, causing local tension, a complete rearrangement is apparently avoided up to a coverage of 0.25, and only every other site in both directions is occupied. A possible model for $\Theta = 0.25$ similar to that proposed by Somerton *et al.*[18] is shown in Fig. 10(a). Because of the high degeneracy of this structure—eight equivalent sites can be occupied—long range order can be easily destroyed by temperature. This situation changes at higher coverages. A structure model for the coverage of 0.5 ML is shown in Fig. 10(b). For this structure basically the same local configurations were assumed as at $\Theta = 0.25$. In order to match the lattice constants of W_2N more closely a contraction of the asymmetrically occupied rows of W atoms in the (001) direction was assumed, the mismatch to the underlying W lattice causing the long superlattice period in this direction. In the other direction a widening of the lattice is again possible only by moving W atoms out of the original plane.

V. SUMMARY AND CONCLUSIONS

We have shown that the dissociative chemisorption of N_2 on W(110) can be greatly enhanced by increasing kinetic energy. This increase follows an S-shaped curve which has been analyzed to yield a barrier height distribution for the dissociation process. Changing incidence angle has little effect on this behavior, indicating a scaling with the total initial kinetic energy, in contrast to the normal kinetic energy scaling predicted by one-dimensional barrier models. We believe that this result arises due to a strong chemical interaction prior to the barrier to dissociation. This interaction may act either to increase the effective surface corrugation or to cause multiple encounters which scramble the parallel and perpendicular motions. Angular distributions reveal a substantial direct-inelastic channel, but a diffuse channel may also be present. We find that even the saturation coverage can be increased with increasing incidence energy, rising from 0.25 ML at low energies to over 0.52 ML at 100 kJ mol^{-1}. This behavior indicates that the effective number of sites for chemisorption is energy dependent.

ACKNOWLEDGMENTS

It is a pleasure to thank J. E. Schlaegel for his many contributions to these experiments and for assistance with the maintenance and upkeep of the apparatus. Two of us (RJM and JL) gratefully acknowledge support of the DOE Office of Basic Energy Sciences (DE-ATO3-79ER10490). We also thank P. S. Bagus, J. W. Gadzuk, and M. J. Cardillo for helpful discussions.

[1] J. E. Lennard-Jones, Trans. Faraday Soc. **28**, 333 (1932).
[2] M. Balooch, M. J. Cardillo, D. R. Miller, and R. E. Stickney, Surf. Soc. **46**, 358 (1974).
[3] M. Balooch and R. E. Stickney, Surf. Sci. **44**, 310 (1974).
[4] M. J. Cardillo, M. Balooch, and R. E. Stickney, Surf. Sci. **50**, 263 (1975).
[5] C. T. Rettner, H. E. Pfnür, and D. J. Auerbach, Phys. Rev. Lett. **54**, 2716 (1985).
[6] C. T. Rettner, L. A. Delouise, and D. J. Auerbach, J. Vac. Sci. Technol. (in press); C. T. Rettner, L. A. Delouise, and D. J. Auerbach, J. Chem. Phys. (in press).
[7] M. P. D'Evelyn, A. V. Hamza, G. E. Gdowski, and R. J. Madix, Surf. Sci. **167**, 451 (1986).
[8] W. van Willigen, Phys. Lett. A **28**, 80 (1968).
[9] J. Arthur and T. Brown, J. Vac. Sci. Technol. **12**, 200 (1975).
[10] G. Comsa, R. David, and B. J. Schumacher, Surf. Sci. **85**, 45 (1979); G. Comsa and R. David, *ibid.* **117**, 77 (1982).
[11] R. P. Thorman and S. L. Bernasek, J. Chem. Phys. **74**, 6498 (1981).
[12] G. D. Kubiak, G. O. Sitz, and R. N. Zare, J. Chem. Phys. **81**, 6397 (1984); **83**, 2538 (1985).
[13] H. P. Steinrück, A. Winkler, and K. D. Rendulic, J. Phys. C **17**, L311 (1984).
[14] Z. W. Gortel, H. J. Kreutzer, G. Wedler, and M. Schäff, Surf. Sci. **143**, 287 (1984).
[15] R. C. Cosser, S. R. Bare, S. M. Francis, and D. A. King, Vacuum **31**, 503 (1981).
[16] T. E. Madey and J. T. Yates, Jr., Nuovo Cimento Suppl. **5**, 486 (1967).
[17] P. W. Tamm and L. D. Schmidt, Surf. Sci. **26**, 286 (1971).
[18] C. Somerton and D. A. King, Surf. Sci. **89**, 391 (1979).
[19] D. J. Auerbach, J. E. Schlaegel, J. Lee, and R. J. Madix, J. Vac. Sci. Technol. A **1**, 1271 (1983).
[20] J. Lee, R. J. Madix, J. E. Schlaegel, and D. J. Auerbach, Surf. Sci. **143**, 626 (1984).
[21] D. J. Auerbach, H. E. Pfnür, C. T. Rettner, J. E. Schlaegel, J. Lee, and R. J. Madix, J. Chem. Phys. **81**, 2515 (1984).
[22] A. W. Kleyn, A. C. Luntz, and D. J. Auerbach, Phys. Rev. Lett. **47**, 1169 (1981); A. C. Luntz, A. W. Kleyn, and D. J. Auerbach, Phys. Rev. B **25**, 4273 (1982); A. W. Kleyn, A. C. Luntz, and D. J. Auerbach, Surf. Sci. **117**, 33 (1982).
[23] C. T. Rettner, L. A. Delouise, J. P. Cowin, and D. J. Auerbach, Faraday Discuss. Chem. Soc. **80**, 1 (1985); C. T. Rettner, L. A. Delouise, J. P. Cowin, and D. J. Auerbach, Chem. Phys. Lett. **118**, 355 (1985).
[24] D. A. King and M. G. Wells, Surf. Sci. **29**, 454 (1972).
[25] M. P. D'Evelyn, H. P. Steinrück, A. Winkler, and R. J. Madix, Surf. Sci. (submitted).
[26] S. L. Tang, M. B. Lee, J. D. Beckerle, M. A. Hines, and S. T. Ceyer, J. Chem. Phys. **82**, 2826 (1985).
[27] K. Besocke and H. Wagner, Surf. Sci. **87**, 457 (1979).
[28] S. P. Singh-Boparai, M. Bowker, and D. A. King, Surf. Sci. **53**, 55 (1975).
[29] D. L. Adams and L. H. Germer, Surf. Sci. **27**, 21 (1971).
[30] R. S. Polizzotti and G. Ehrlich, J. Chem. Phys. **71**, 259 (1979).
[31] R. A. Oman, J. Chem. Phys. **48**, 3919 (1968).
[32] D. R. Miller and R. B. Subbarao, J. Chem. Phys. **52**, 425 (1970).
[33] R. B. Subbarao and D. R. Miller, J. Chem. Phys. **58**, 5247 (1973).
[34] S. M. Lui, W. E. Rodgers, and E. L. Knuth, *Rarefied Gas Dynamics*, edited by M. Becker and M. Fiebig (DFVRL, Porz-Wahn, Germany, 1974), p. E. 8-1.
[35] J. E. Hurst, L. Wharton, K. C. Janda, and D. J. Auerbach, J. Chem. Phys. **78**, 1559 (1983).
[36] T. A. Delchar and G. Ehrlich, J. Chem. Phys. **42**, 2686 (1965).
[37] J. T. Yates, Jr., R. Klein, and T. E. Madey, Surf. Sci. **58**, 469 (1976).
[38] E. Umbach, A. Schichl, and D. Menzel, Solid State Commun. **36**, 93 (1980).
[39] A. Schichl, D. Menzel, and N. Rösch, Chem. Phys. **65**, 225 (1982).
[40] J. T. Yates, Jr. and T. E. Madey, Surf. Sci. **28**, 437 (1971).
[41] J. W. Gadzuk and S. Holloway, Chem. Phys. Lett. **114**, 314 (1985); S.

Holloway and J. W. Gadzuk, J. Chem. Phys. **82**, 5203 (1985).
[42]See also: J. K. Nørskov and B. I. Lundqvist, Surf. Sci. **89**, 251 (1979); B. Kasemo and I. B. Lundqvist, Comments At. Mol. Phys. **14**, 229 (1984), and references therein.
[43]E. Bauer (private communication).
[44]K. P. Huber and G. Herzberg, *Molecular Spectra and Molecular Structure: IV. Constants of Diatomic Molecules* (Van Nostrand, New York, 1979).
[45]P. S. Bagus (private communication).
[46]J. W. Gadzuk, J. Chem. Phys. **79**, 6341 (1983).
[47]E. E. Nikitin, and L. Zukicke, *Selected Topics of the Theory of Chemical Elementary Processes* (Springer, Berlin, 1982).
[48]C. W. Muhlhasen, J. A. Seri, J. C. Tully, G. E. Becker, and M. J. Cardillo, Isr. J. Chem. **22**, 315 (1982).
[49]H. Asada, Jpn. J. Appl. Phys. **20**, 527 (1981).
[50]K. C. Janda, J. E. Hurst, J. Cowin, L. Wharton, and D. J. Auerbach, Surf. Sci. **130**, 395 (1983).
[51]See, for example: J. A. Barker and D. J. Auerbach, Surf. Sci. Rep. **4**, 1 (1985).
[52]D. A. King, CRC Crit. Rev. Solid State Mater. Sci. **7**, 167 (1978), and references therein.
[53]P. Kisliuk, J. Phys. Chem. Solids **3**, 75 (1957).
[54]A. Yoshimori and Y. Odoi, Surf. Sci. **143**, 37 (1984).
[55]V. I. Khitrova and Z. G. Pinsker, Sov. Phys. Crystallogr. **6**, 712 (1962).